MATHDISCOVERIES
Mathematical Preprint

Working Draft

The Volume–Determinant Inequality for Alternating Hyperbolic Knots with Seven and Eight Twist Regions

Tyler B. Hughes*,†

†Independent Researcher, United States

S *Supporting Information:* `recompute.py` *verifier and trust-boundary ledgers (no Lean 4)*

Disclosure: AI-assisted working draft directed by Tyler B. Hughes. Not for submission as is. No human mathematician has yet refereed the proof.

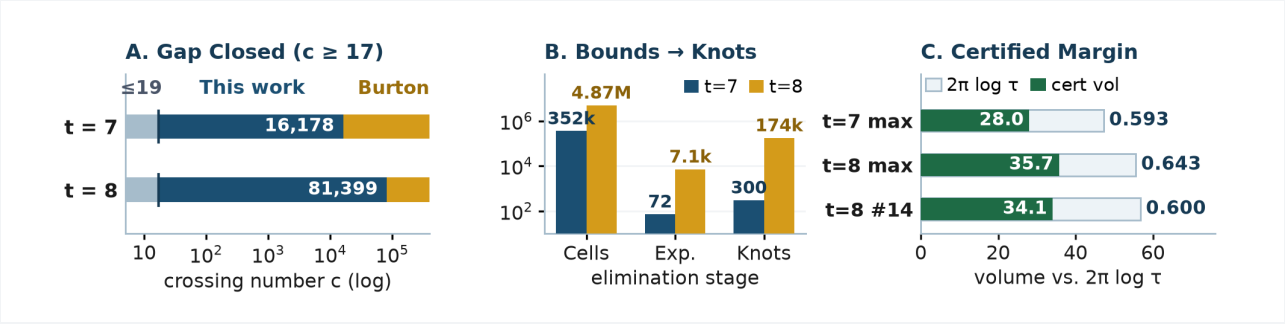

ABSTRACT: Champanerkar, Kofman, and Purcell (2016) conjectured $\mathrm{vol}(K) < 2\pi \log \det(K)$ for every alternating hyperbolic knot K and checked $c \le 16$; asymptotic bounds start at $c \ge 16{,}178$ ($t = 7$) and 81,399 ($t = 8$) (Burton 2018) or need $t > 8$ (Egorov–Vesnin 2026). We settle the inequality for every alternating hyperbolic knot with 7 twist regions and $c \ge 17$, and for every alternating hyperbolic knot with 8 twist regions and $c \ge 17$, given that SnapPy's verified computation encloses the volume of the knot diagram supplied. A general-t nerve upper bound $\mathrm{vol}(K) < 2(6t - 2 - D_{\max})G$, Adams's bigon-chain bound, and tree-mean determinant bounds lower every $c \ge 17$ configuration to finite critical cells. At $t = 7$, Tutte-matched enumeration (408 rootings) eliminates 351,521 of 351,593 cells and leaves 300 residual knots, all SnapPy-certified (max ratio 0.5933). At $t = 8$, enumeration (1,938 rootings) eliminates 4,860,736 of 4,867,828 cells and leaves 173,628 residual knots, all SnapPy-certified (max ratio 0.6430). Links, $c \le 16$, and $T_J \ge 9$ are not claimed; no Lean 4 formalization is claimed.

Verification Scope (G11): WARN: Human referee: pending
Main results: 0 of 5 in Lean Kernel (0%) · 2 Cert Only · 3 written · 1 open (not counted)
Abstract claims: 0 of 7 in Lean Kernel (0%) · 4 Cert Only · 3 written

Full Trust Boundary: Section 5.

MSC 2020: 57K10, 57K32, 05C30 **Keywords:** alternating knots, hyperbolic volume, knot determinant, twist regions, planar maps, verified interval arithmetic

1. INTRODUCTION AND MAIN RESULTS

A reduced alternating diagram D of a prime alternating knot $K \subset S^3$ decomposes naturally into *twist regions*, maximal runs of crossings where two strands twist around one another. The number of twist regions of a prime, twist-reduced alternating diagram is a knot invariant $T_J(K)$ equal to the sum of the absolute values of the second and penultimate coefficients of the Jones polynomial [10, 8]. Champanerkar, Kofman, and Purcell [5] (Conjecture 1.10) conjectured that every alternating hyperbolic knot K satisfies the *volume–determinant inequality* (Vol–Det),

$$\mathrm{vol}(K) < 2\pi \log \det(K), \tag{1}$$

showed that the constant 2π is asymptotically sharp (Corollary 1.11 of [5]), and verified (1) experimentally for all alternating knots through 16 crossings.

Subsequent work established (1) on several structured families and asymptotic regimes. Burton [4] proved Vol–Det for all 2-bridge links (Theorem 3.5), alternating closed 3-braids (Theorem 4.1), alternating pretzel links with at most 13 twist columns (§5.1, computer-assisted), and highly twisted alternating links satisfying $c \ge t + \xi^{t-1} - 2\gamma^{t-1}$ (Theorem 5.1), where $\xi = \exp(5v_3/\pi) \approx 5.0295461$ and $\gamma \approx 1.4252996$. At $t = 7$ and $t = 8$ twist regions, Burton's Theorem 5.1 starts at $c \ge 16{,}178$ and $c \ge 81{,}399$ crossings, respectively. Egorov and Vesnin [7] (Theorem 1) lowered the asymptotic crossing threshold substantially, but their hypothesis requires $t(D) > 8$ twist regions, leaving $t = 7$ and $t = 8$ untouched. At small crossing numbers, Stanggassinger [11] reported an unrefereed computation verifying Vol–Det for prime alternating knots through 19 crossings. Between 20 crossings and Burton's thresholds (16,178 at $t = 7$ and 81,399 at $t = 8$), the prior-work searches logged in Section 6 located no source settling either twist-number class.

We close the entire gap from $c = 17$ onward for alternating hyperbolic knots with seven or eight twist regions, subject to one explicit software trust condition.

Theorem 1 (Vol–Det for Seven Twist Regions, $c \geq 17$). *Every alternating hyperbolic knot K with twist number $T_J(K) = 7$ and crossing number $c(K) \geq 17$ satisfies*

$$\mathrm{vol}(K) < 2\pi \log \det(K),$$

given that SnapPy's verified volume computation inside SageMath encloses the hyperbolic volume of the knot whose diagram it is given.

Theorem 2 (Vol–Det for Eight Twist Regions, $c \geq 17$). *Every alternating hyperbolic knot K with twist number $T_J(K) = 8$ and crossing number $c(K) \geq 17$ satisfies*

$$\mathrm{vol}(K) < 2\pi \log \det(K),$$

given that SnapPy's verified volume computation inside SageMath encloses the hyperbolic volume of the knot whose diagram it is given.

Both theorems are computer-assisted and strictly scoped. Nothing is claimed at $c \leq 16$ crossings (which rests on Champanerkar, Kofman, and Purcell's experimental check [5] and is not re-evaluated here), nothing is claimed for multi-component alternating links (358 residual link rows at $t = 7$ and 244,170 at $t = 8$ were filtered out by determinant parity without computing volumes), and nothing is claimed for $T_J(K) \geq 9$ (where a separate nine-region computation has an unresolved review issue). No Lean 4 formalization is claimed in this manuscript.

Figure 1 summarizes the four-stage proof architecture. Every prime, twist-reduced alternating diagram D with t twist regions compresses to a loopless 2-connected plane multigraph H with t edges, an assignment of each edge as a parallel *bundle* or series *path*, and a vector $a = (a_1, \ldots, a_t)$ of twist-region crossing counts summing to $c = \sum_e a_e$. The knot determinant $\det(K)$ equals a weighted spanning-tree sum $\tau(a)$ on H, which increases monotonically in every a_e. On the volume side, we combine two diagram-dependent upper bounds: a general-t *nerve bound* $\mathrm{vol}(K) < 2(6t - 2 - D_{\max})G$ derived from the right-angled ideal polyhedron of the fully augmented link (Lemma 3), where $G = 0.915965594\ldots$ is Catalan's constant, and Adams's *bigon-chain bound* (BCB, Theorem 3.1 of [1]).

Because BCB saturates once every twist region has at least 5 crossings and the nerve bound is independent of all twist sizes $a_e \geq 2$, monotonicity of $\tau(a)$ lowers all configurations with $c \geq 17$ to a finite collection of *critical cells* (Lemma 5). Over 99.97% of cells at $t = 7$ and over 99.85% at $t = 8$ are settled immediately by two closed-form AM–GM lower bounds on τ (Lemma 4). Expanding the few undecided critical cells upward row by row terminates with 0 cells cut, leaving only 300 knot rows at $t = 7$ and 173,628 at $t = 8$ for direct SnapPy volume certification (Propositions 6 and 7).

Concept in Action: 7- and 8-Bond Check (`recompute.py`)

```
import math
v3 = 1.0149416064096536
def check_bond(sz):
    tau = sum(math.prod(sz[j] for j in range(len(sz))
              if j != i) for i in range(len(sz)))
    w = {2: 6*v3, 3: 7.855, 4: 9.2376}
    c = {2: 11*v3, 3: 10.087, 4: 10.2872}
    bcb = sum(w.get(k, 10*v3) for k in sz) - c.get(max(sz), 12.11)
    return tau, round(bcb, 2), round(2*math.pi*math.log(tau), 2)
# (5,2,2,2,2,2,2) -> (1024, 34.58, 43.55)  # BCB < 2 pi log tau
# (3,2,2,2,2,2,2,2) -> (1472, 40.4, 45.83) # link (even tau)
```

The remainder of the paper is organized as follows. Section 2 fixes the plane-map reduction, spanning-tree determinant formula, and worked 7-bond and 8-bond examples. Section 3 proves the three written reduction lemmas (Lemmas 3–5) and tabulates the nerve thresholds $B_t(D)$ for $t \in \{7, 8\}$. Section 4 reports the Tutte-matched map enumeration, cell elimination, residual SnapPy certifications (including the 14 direct certificates and reflection-twin confirmation closing the final $t = 8$ knot), proofs of Theorems 1 and 2, and the open scope (Conjecture 8). Section 5 presents the machine-generated Reader's Trust Boundary, Section 6 reviews prior work and logged search gaps, and Section 7 documents data availability and AI disclosure.

2. DEFINITIONS, TWIST-REGION MAPS, AND WORKED EXAMPLES

Let $D \subset S^2$ be a reduced, prime, twist-reduced alternating diagram of a hyperbolic link K with $c = c(D)$ crossings and $t = t(D) \geq 3$ twist regions, in the sense of Lackenby [10] and Futer, Kalfagianni, and Purcell [8, 9]. Recall that a *twist region* is a maximal chain of bigon faces arranged end-to-end (or a single crossing adjacent to no bigon), and D is *twist-reduced* if every simple closed curve meeting D transversely in four points adjacent to two crossings bounds a region containing a (possibly empty) string of bigons between those two crossings. By Menasco's theorem and the twist-reduction theorem [10, 8], every prime alternating hyperbolic knot K with $T_J(K) = t$ admits a prime, twist-reduced alternating diagram D with $t(D) = t$ and $c(D) = c(K)$ crossings.

Checkerboard graphs and reduction plane maps. Two-color the complementary regions of D on S^2 in checkerboard fashion (black and white), and form the black checkerboard (Tait) graph G: one vertex per black region and one edge per crossing joining the two incident black regions. Because D is prime and reduced, G is a loopless, 2-connected plane multigraph with c edges. Each twist region of $a_e \geq 1$ crossings corresponds in G either to a *bundle* of a_e parallel edges sharing the same two vertices (labelled b) or to a *path* of a_e edges in series separated by degree-2 vertices (labelled p); a single crossing ($a_e = 1$) can be viewed as either a bundle or a path. Replacing each bundle by one edge and each maximal path of degree-2 vertices by one edge collapses G to its *reduction plane map* H, a loopless 2-connected plane multigraph on n vertices with t edges and $f = t + 2 - n$ faces.

Conversely, a *configuration* (H, s, a) specifies a loopless 2-connected t-edge plane map H, a labelling $s \in \{\mathrm{b}, \mathrm{p}\}^t$, and

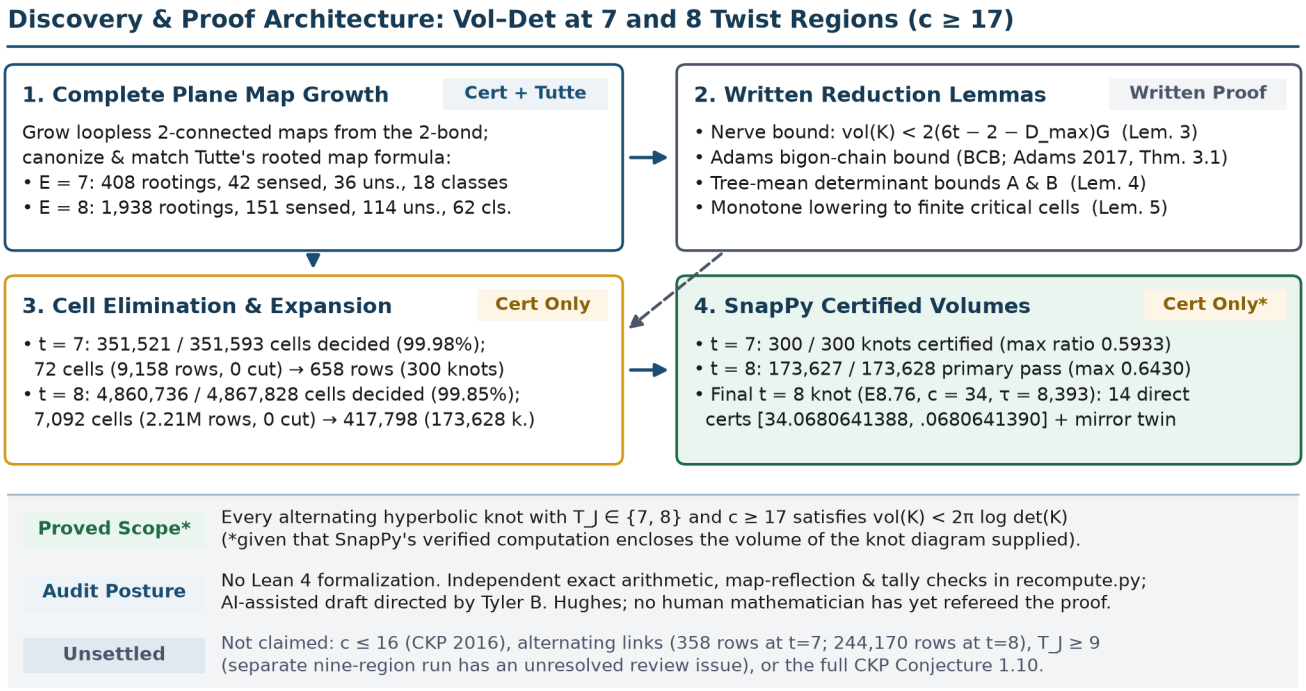

Figure 1. Discovery and proof architecture for Theorems 1 and 2. Complete plane-map enumeration matched against Tutte's formula [13] (`[to check]`) and three written reduction lemmas (Lemmas 3–5) eliminate over 99.85% of critical cells algebraically, leaving finite residual knot lists settled by SnapPy verified volume enclosures inside SageMath. Explicitly unsettled boundaries appear in the flat borderless footer row.

integer twist sizes $a = (a_1, \dots, a_t) \in \mathbb{Z}^t_{\geq 1}$ with $c = \sum_{e=1}^{t} a_e$, reconstructing G by replacing each edge e by a_e parallel edges (if $s_e = \mathrm{b}$) or a subdivided path of a_e edges (if $s_e = \mathrm{p}$). A *part* (H, s, S_1) fixes H, s, and the subset $S_1 \subseteq \{e : s_e = \mathrm{b}\}$ of edges held at a single crossing ($a_e = 1$), with every remaining (*free*) edge satisfying $a_e \geq 2$. A part is *twist-reduced* if (i) no two edges with $a_e = 1$ (or an $a_e = 1$ edge and a path) meet at a degree-2 vertex of H (which would merge two twist regions), and (ii) no two bundle-or-single edges share the same endpoints in H and no two path-or-single edges separate the same pair of faces of H (which would admit a flype reducing the twist number below t). Replacing G by its planar dual G^* swaps $\mathrm{b} \leftrightarrow \mathrm{p}$ on the dual map H^* without changing D, and reflecting S^2 yields the mirror-image diagram with identical hyperbolic volume and determinant. Thus it suffices to analyze one representative map H from each equivalence class of loopless 2-connected t-edge plane maps up to planar duality and mirror reflection.

Determinant as a weighted spanning-tree sum. For any reduced alternating diagram D with checkerboard graph G, the determinant equals the number of spanning trees of G, $\det(K) = \tau(G)$ (Stoimenow [12] `[to check]`, cited via Burton [4], p. 4). Contracting or deleting each expanded twist region expresses $\tau(G)$ directly in terms of the spanning-tree set $\mathcal{T}(H)$ of the t-edge reduction map H:

$$\tau(a) := \tau(G) = \sum_{T \in \mathcal{T}(H)} \prod_{e \in A(T)} a_e, \tag{2}$$

where the *active set* $A(T)$ of a spanning tree $T \in \mathcal{T}(H)$ consists of all bundle edges lying *in* T together with all path edges lying *outside* T. Indeed, a spanning tree of G selects one of the a_e parallel edges from each bundle $e \in T$ (and none from $e \notin T$), while omitting one of the a_e series edges from each path $e \notin T$ (and retaining all a_e edges from $e \in T$). Single crossings ($a_e = 1$) contribute factor 1 in every term. Moreover, a knot has odd determinant whereas any alternating link of two or more components has even determinant, so the parity of $\tau(a)$ partitions residual diagrams cleanly into knots (τ odd) and links (τ even).

Worked hand examples at $t = 7$ and $t = 8$. To illustrate (2) and the interplay between the two volume bounds, consider the t-bond $H = B_t$ (two vertices joined by t parallel edges) with every twist region a path ($s = \mathrm{p}^t$). Each of the t spanning trees of B_t consists of a single edge e_i, so its active set is the complement $\{1, \dots, t\} \setminus \{i\}$ and $\tau(a) = \sum_{i=1}^{t} \prod_{j \neq i} a_j$.

- *Seven-bond example* ($c = 17$, *knot/link parity check*). Take $t = 7$ with sizes $(5, 2, 2, 2, 2, 2, 2)$ ($c = 17$). The spanning tree omitting the size-5 edge contributes $2^6 = 64$, and the six trees omitting a size-2 edge contribute $5 \cdot 2^5 = 160$ each, giving

$$\tau = 64 + 6 \cdot 160 = 1{,}024, \qquad 2\pi \log \tau \approx 43.5517.$$

Adams's bigon-chain bound (Section 3) gives $6(6v_3) + 10v_3 - 12.110 \approx 34.5773 < 43.5517$, deciding the configuration immediately. By contrast, its nerve has $D_{\max} = 11$, yielding nerve bound $2(40 - 11)G \approx 53.1260$ and thresh-

old $B_7(11) = 4{,}699 > 1{,}024$, so the nerve bound alone does not decide it.

- *Eight-bond example* ($c = 17$, *even* τ*: link*). Take $t = 8$ with sizes $(3,2,2,2,2,2,2,2)$ ($c = 17$). Then

$$\tau = 2^7 + 7 \cdot 3 \cdot 2^6 = 128 + 7 \cdot 192 = 1{,}472,$$
$$2\pi \log \tau \approx 45.8319.$$

Here $\tau = 1{,}472$ is even (so this diagram is a link rather than a knot; it illustrates the arithmetic of both bounds, which hold for all alternating hyperbolic links). Adams's bigon-chain bound gives $7(6v_3) + 7.855 - 10.087 \approx 40.3955 < 45.8319$, deciding the diagram, whereas its nerve has $D_{\max} = 12$ (each vertex of B_8 meets all 8 faces and each face meets both vertices and its 2 neighboring faces, so $8 + 4 = 12$), giving nerve bound $2(46 - 12)G \approx 62.2857$ and $B_8(12) = 20{,}192 > 1{,}472$.

3. ANALYTICAL VOLUME BOUNDS AND FINITE REDUCTION

We establish the three written lemmas that reduce all 7- and 8-twist-region alternating hyperbolic diagrams with $c \geq 17$ crossings to finite candidate lists.

Lemma 3 (General-t Nerve Upper Bound). *Let D be a prime, twist-reduced alternating diagram of a hyperbolic link K with $t \geq 3$ twist regions, reduction plane map H, and twist-reduced part (H, s, S_1). Let N be the triangulation of S^2 obtained from the radial graph of H (whose vertices are the n vertices and f faces of H, joined along corners) by inserting in each edge quadrilateral the edge of H if $s_e = \mathrm{b}$, its dual edge if $s_e = \mathrm{p}$, and either diagonal if $e \in S_1$, choosing the assignment on S_1 that maximizes*

$$D_{\max} := \max_{uv \in E(N)} (\deg_N(u) + \deg_N(v)).$$

Then

$$\mathrm{vol}(S^3 \backslash K) < 2(6t - 2 - D_{\max})\, G, \tag{3}$$

where $G = \sum_{k=0}^{\infty} (-1)^k/(2k+1)^2 \approx 0.915965594$ is Catalan's constant. Consequently, if

$$\det(K) > B_t(D_{\max}) := \left\lfloor \exp\left(\frac{(6t - 2 - D_{\max})G}{\pi} \right) \right\rfloor,$$

then K satisfies (1).

Proof. Encircle each twist region of D by a crossing circle and remove full twists to obtain a fully augmented link L whose complement $S^3 \backslash L$ is homeomorphic to the complement of K together with the crossing circles [9] (Figure 2). Filling each crossing circle along its meridian recovers $S^3 \backslash K$, so by Thurston's hyperbolic Dehn filling theorem [9] (Theorem 4.3), $\mathrm{vol}(S^3 \backslash K) < \mathrm{vol}(S^3 \backslash L)$.

Because D is prime and twist-reduced, $S^3 \backslash L$ is hyperbolic and decomposes into two copies of a single right-angled ideal polyhedron P cut out by an orthogonal circle packing on S^2 whose nerve is a triangulation [9] (§3.1.2) and whose faces are checkerboard colored white (projection plane regions outside bigons) and dark (bow-tie pairs of triangles in the twice-punctured crossing disks) [10] (Agol–D. Thurston appendix). Thus $\mathrm{vol}(S^3 \backslash L) = 2\,\mathrm{vol}(P)$.

The white faces of P correspond to the n vertices and f faces of H, giving $n + f = t + 2$ vertices of the nerve N by Euler's formula. Each ideal vertex of P corresponds to an edge of N: the $2t$ corners of H (separating a vertex from an incident face) together with t crossing-circle diagonals—joining the endpoints of e for a bundle, the adjacent faces of e for a path, and either pair at a single crossing $e \in S_1$ (since a crossing circle may encircle either opposite pair of regions at a single crossing). Because (H, s, S_1) is twist-reduced, no two diagonals coincide, so N is a simple triangulation of S^2 with $t + 2$ vertices and $3t$ edges.

Accordingly, P is a 4-valent right-angled ideal polyhedron with $V = 3t$ ideal vertices and $6t$ edges. Place the ideal vertex v of P corresponding to an edge $uv \in E(N)$ of maximum degree sum $D_{\max} = d_1 + d_2$ at ∞ in upper half-space $\mathbb{H}^3$. The four faces incident to v become vertical planes (two dark triangles and two parallel white faces of d_1 and d_2 ideal vertices), while every other face lies on a hemisphere orthogonal to adjacent hemispheres. Coning P from v decomposes P into pairs of orthoschemes over the edges e of P between two hemispheres; by Milnor's orthoscheme formula (Atkinson [3], p. 13; Alexandrov, Bogachev, Egorov, and Vesnin [2], p. 9), an edge where orthogonal hemispheres meet contributes $\Lambda(\theta_e) + \Lambda(\pi/2 - \theta_e)$ with $\theta_e \in (0, \pi/2)$, where $\Lambda(\theta) = -\int_0^\theta \log|2 \sin u|\, du$ is Lobachevsky's function. Since $\frac{d}{d\theta}[\Lambda(\theta) + \Lambda(\pi/2 - \theta)] = \log \cot \theta$ vanishes uniquely at $\theta = \pi/4$, each such edge contributes at most $2\Lambda(\pi/4) = G = v_8/4$ [3] (p. 3).

Of the $6t$ edges of P, exactly 4 meet v, 1 lies opposite v on each of the two dark triangles at v, and $(d_1 - 2) + (d_2 - 2)$ lie on the bases of the two white faces at v (disjoint from the dark triangles and from each other because the two white faces at ∞ are parallel vertical planes). Hence the number of hemisphere–hemisphere edges is

$$6t - 4 - 1 - 1 - (d_1 - 2) - (d_2 - 2) = 6t - 2 - D_{\max},$$

yielding $\mathrm{vol}(P) \leq (6t - 2 - D_{\max})G$ (equivalently, Lemma 3.2 of [2] with $V = 3t$ and $m = (d_1 - 3) + (d_2 - 3) = D_{\max} - 6$ quasi-adjacent vertices at v, giving $(V - 4 - m/2)\, v_8/2 = (6t - 2 - D_{\max})G$). Doubling gives $\mathrm{vol}(S^3 \backslash K) < 2\,\mathrm{vol}(P) \leq 2(6t - 2 - D_{\max})G$. Taking exponentials of $(6t - 2 - D_{\max})G/\pi$ gives the integer threshold $B_t(D_{\max})$. □

Table 1 records the exact nerve bounds and determinant thresholds $B_t(D)$ for $t = 7$ ($D = 10, \ldots, 16$) and $t = 8$ ($D = 10, \ldots, 18$), verified to 60 decimal digits in `recompute.py`. Note the identity $B_8(D + 6) = B_7(D)$ since $46 - (D + 6) = 40 - D$. Across $D \in \{10, \ldots, 16\}$ at $t = 7$, every exponential $\exp((40 - D)G/\pi)$ lies at distance at least 0.1389 from the nearest integer (and at least 0.0809 across $D \in \{10, \ldots, 18\}$ at $t = 8$), eliminating any rounding ambiguity.

Adams's bigon-chain bound. Alongside Lemma 3, we use Theorem 3.1 of Adams [1]: for any hyperbolic alternating link L (other than the Borromean rings) in a reduced, twist-reduced alternating diagram with $c \geq 5$ crossings and at least 3 twist regions, letting t_i count twist regions of exactly i crossings and g_5 count those of at least 5 crossings,

$$\mathrm{vol}(S^3 \backslash L) < \sum_{e=1}^{t} w(a_e) - \alpha(\max_e a_e), \tag{4}$$

where $w(1) = v_8 = 4G \approx 3.66386$, $w(2) = 6v_3 \approx 6.08965$, $w(3) = 7.8549\ldots$, $w(4) = 9.2375\ldots$, $w(k) = 10v_3 \approx 10.14942$

Table 1. Nerve upper bounds $2(6t-2-D)G$ and determinant thresholds $B_t(D) = \lfloor \exp((6t-2-D)G/\pi) \rfloor$ for $t = 7$ and $t = 8$ (verified to 60 digits in `recompute.py`).

D	$2(40-D)G$	$B_7(D)$	$2(46-D)G$	$B_8(D)$
10	54.957936	6,290	65.949523	36,177
11	53.126004	4,699	64.117592	27,028
12	51.294073	3,511	62.285660	20,192
13	49.462142	2,623	60.453729	15,085
14	47.630211	1,959	58.621798	11,270
15	45.798280	1,464	56.789867	8,420
16	43.966349	1,093	54.957936	6,290
17	—	—	53.126004	4,699
18	—	—	51.294073	3,511

for $k \geq 5$ (with $v_3 = 3\Lambda(\pi/3) \approx 1.0149416$ the volume of the regular ideal tetrahedron), and the subtracted constant is $\alpha(1) = 15.4972$, $\alpha(2) = 11v_3 \approx 11.16436$, $\alpha(3) = 10.088$, $\alpha(4) = 10.2873$, and $\alpha(k) = 12.111$ for $k \geq 5$. In every automated check, decimal weights are rounded strictly *up* (7.855, 9.2376) and subtracted constants strictly *down* (15.4971, 10.087, 10.2872, 12.110), so every decision made by (4) is strictly conservative. Weight by weight, Adams's BCB strictly improves Dasbach and Tsvietkova's bound [6] (Theorem 2.3).

Lemma 4 (Weighted Spanning-Tree Determinant Lower Bounds). *Fix a twist-reduced part (H, s, S_1) with $N = |\mathcal{T}(H)|$ spanning trees and free-edge set $F = \{1, \dots, t\} \setminus S_1$. For any size vector a with $a_e = 1$ $(e \in S_1)$ and $a_e \geq 2$ $(e \in F)$, let $m_e = |\{T \in \mathcal{T}(H) : e \in A(T)\}|$, and partition $\mathcal{T}(H) = \bigsqcup_k \mathcal{T}_k$ by the number $k = |A(T) \cap F|$ of active free edges, setting $p_k = |\mathcal{T}_k|$ and $m_{k,e} = |\{T \in \mathcal{T}_k : e \in A(T)\}|$. Then:*

1. (Bound A) $\tau(a) \geq N \prod_{e \in F} a_e^{m_e/N}$.
2. (Bound B) $\tau(a) \geq \sum_{k : p_k > 0} p_k \prod_{e \in F} a_e^{m_{k,e}/p_k}$.
3. (Placement minimization) *For any fixed multiset M of $|F|$ free sizes, each product $\prod_{e \in F} a_e^{m_e/N}$ or $\prod_{e \in F} a_e^{m_{k,e}/p_k}$ is minimized over all assignments of M to F by sorting sizes in decreasing order against exponents in increasing order.*

Proof. Write $\tau(a) = \sum_{T \in \mathcal{T}(H)} t_T$, where each term $t_T = \prod_{e \in A(T) \cap F} a_e$ is strictly positive. Applying the AM–GM inequality over all N trees yields

$$\tau(a) \geq N \Bigg(\prod_{T \in \mathcal{T}(H)} t_T \Bigg)^{1/N} = N \prod_{e \in F} a_e^{m_e/N},$$

which is Bound A. Applying AM–GM separately inside each nonempty class $\mathcal{T}_k$ yields

$$\sum_{T \in \mathcal{T}_k} t_T \geq p_k \Bigg(\prod_{T \in \mathcal{T}_k} t_T \Bigg)^{1/p_k} = p_k \prod_{e \in F} a_e^{m_{k,e}/p_k},$$

and summing over k gives Bound B. Finally, taking logarithms converts $\prod_{e \in F} a_e^{\beta_e}$ into $\sum_{e \in F} \beta_e \log a_e$, which by the rearrangement inequality is minimized over all bijections between M and F when the values $\log a_e$ are ordered oppositely to the exponents β_e. □

Because each class in Bound B is minimized independently over placements, a single placement may not realize all class minima simultaneously, so the elimination script takes the maximum of integer-floored Bound A and Bound B (computed by exact integer p_k-th roots) for each cell (H, s, S_1, M).

Lemma 5 (Monotonicity and Finite Critical Reduction). *Fix a twist-reduced part (H, s, S_1) and a threshold $c_{\min} = 17$. Define a* critical cell *to be a multiset M of $|F|$ free sizes ≥ 2 such that either (i) every entry of M lies in $\{2, 3, 4, 5\}$ and $|S_1| + \sum_{x \in M} x \geq 17$, or (ii) $|S_1| + \sum_{x \in M} x = 17$ with at least one entry ≥ 6. Then:*

1. *Every configuration (H, s, S_1, a) with $c = \sum_e a_e \geq 17$ reduces by decrementing entries ≥ 6 to a configuration whose multiset of free sizes is a critical cell, without increasing $\tau(a)$ or decreasing either the nerve bound (3) or Adams's BCB (4). Hence if either bound decides a critical cell for every placement of M, it decides every configuration descending to that cell.*
2. *For any critical cell not decided by Bounds A and B, evaluating exact $\tau(a)$ on each placement of M and recursively incrementing any coordinate $a_e \geq 5$ by 1 (stopping along a branch once the nerve bound or BCB holds) decides all but finitely many configurations in that cell.*

Proof. By (2), $\tau(a)$ is a multi-affine polynomial in the free sizes a_e with non-negative integer coefficients, and every edge e of a loopless 2-connected map H lies in at least one spanning tree and misses at least one spanning tree (since H has no bridges and no loops). Therefore $\tau(a)$ is strictly increasing in every coordinate a_e. Decreasing a twist size $a_e \geq 6$ by 1 preserves the part (H, s, S_1) and its nerve $D_{\max}$, leaves the BCB weight $w(a_e) = 10v_3$ and subtraction $\alpha(\max a) = 12.111$ unchanged (since $\max a \geq 5$ before and after), and strictly decreases $\tau(a)$. Repeating until either $c = 17$ or $\max_e a_e \leq 5$ reaches a critical cell in finitely many steps, proving (1).

For (2), fixing any configuration a with $a_e \geq 5$ and incrementing $a_e \mapsto a_e + 1$ strictly increases $\tau(a)$ by at least 1 while leaving both $2(6t - 2 - D_{\max})G$ and BCB constant. Since $2\pi \log \tau(a) \to \infty$ as any coordinate grows, every upward branch crosses $B_t(D_{\max})$ in finitely many steps, so breadth-first expansion halts with a complete finite list of undecided configurations. □

Figure 2 contrasts the two upper bounds against $2\pi \log \tau$ and certified volumes on both the worked 7-bond / 8-bond examples and the tightest residual knots encountered at $t = 7$ and $t = 8$.

4. MAP ENUMERATION, ELIMINATION, AND CERTIFIED VOLUMES

Complete plane-map enumeration against Tutte's formula. Every loopless 2-connected plane map with $E \geq 3$ edges arises from a loopless 2-connected plane map with $E - 1$ edges by either subdividing an edge or inserting an edge across a face between two distinct vertices. Starting from the unique 2-bond, the enumeration script grows all sensed (orientation-preserving) plane maps inductively through $E = 8$ edges, deduplicates them by minimum dart-relabelling canonical code, checks Euler's formula $V - E + F = 2$, 2-connectivity, looplessness, and closure under planar duality and mirror reflection, and sums the orbit-stabilizer rootings $\sum_M 2E/|\mathrm{Aut}^+(M)|$.

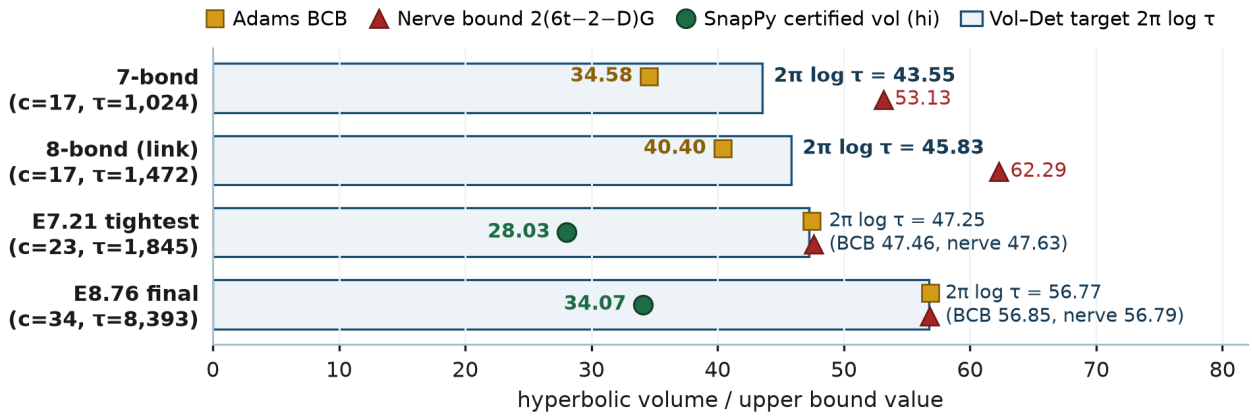

Figure 2. Comparison of Adams's bigon-chain bound (BCB, gold squares), the nerve upper bound $2(6t-2-D_{\max})G$ (red triangles), the Vol–Det threshold $2\pi\log\tau$ (shaded navy bars), and SnapPy certified volume upper ends (green circles) on four concrete configurations. On the worked 7-bond and 8-bond examples, BCB lies well below $2\pi\log\tau$ while the nerve bound sits above it. On the residual knots of E7.21 and E8.76, both upper bounds lie slightly above $2\pi\log\tau$, whereas the certified hyperbolic volumes sit roughly 36%–41% below the threshold.

By Tutte's census formula [13] (`[to check]`, read via OEIS `A000139`), the number of rooted nonseparable planar maps with $E \geq 2$ edges is

$$R(E) = \frac{2(3E-3)!}{E!\,(2E-1)!}. \tag{5}$$

Because orientation-preserving automorphisms of a connected map act freely on its $2E$ darts, a list of distinct sensed nonseparable E-edge maps is complete if and only if $\sum_M 2E/|\mathrm{Aut}^+(M)| = R(E)$. For $E = 2,\dots,8$, `recompute.py` confirms $R(E) = 1, 2, 6, 22, 91, 408, 1{,}938$, and the enumeration matches $R(E)$ exactly at every level, as well as the OEIS `A006402` (sensed) and `A006403` (unsensed, up to mirror image) counts: 16 sensed, 15 unsensed, 9 classes at $E = 6$; 42 sensed, 36 unsensed, 18 classes at $E = 7$; and 151 sensed, 114 unsensed, 62 classes at $E = 8$. Running the same elimination pipeline at $E = 6$ serves as a full regression control: it recovers all 9 classes, 1,541 twist-reduced parts $(13+45+49+105+125+125+125+225+729)$, and 54,813 critical cells, deciding all 54,813 (36,787 by the nerve bound and 18,026 by BCB) with 0 residual rows.

Proposition 6 (Seven-Region Elimination and Residual Certification). *Across the* 18 *duality-and-mirror classes of* 7*-edge loopless* 2*-connected plane maps* (5,670 *twist-reduced parts,* 351,593 *critical cells at* $c \geq 17$*), Bounds A and B decide* 351,521 *cells* (182,358 *by the nerve bound and* 169,163 *by BCB*)*. Upward row-by-row expansion of the remaining* 72 *cells inspects* 9,158 *rows with* 0 *cells cut and leaves exactly* 658 *residual rows, all on map class* E7.21 *at* $D_{\max} = 14$ ($B_7(14) = 1{,}959$, $20 \leq c \leq 25$)*:* 300 *knot rows* $(80+80+52+16+72 = 300$ *for* $c = 21,\dots,25$*;* 0 *at* $c = 20$*) and* 358 *link rows* (250 *of two components and* 108 *of three*)*. Every one of the* 300 *residual knots passes exact determinant, alternating, component, and twist-region checks and receives a certified SnapPy volume enclosure satisfying* (1)*, with largest volume-to-bound ratio*

$$\frac{\mathrm{vol}_{\mathrm{hi}}}{2\pi\log\tau} = \frac{28.032822531009273}{47.25102727178557} \approx 0.5933$$

attained at E7.21*, labelling* `pppppbpp`*, sizes* $(3,3,3,4,3,3,4)$*,* $c = 23$*,* $\tau = 1{,}845$*.*

All 658 residual rows at $t = 7$ lie on a single map class, represented by E7.21 (five vertices of degrees $(2,3,3,3,3)$, four faces of sizes $(3,3,4,4)$, and 24 spanning trees, verified independently in `recompute.py` alongside the plant knot `pppppbpp` at $(3,3,3,3,3,4,4)$ with $\tau = 1{,}855$, the tightest knot $\tau = 1{,}845$, and the plant link `bbpppppp` with single crossing on edge 1 and sizes $(2,1,4,4,4,4,4)$ giving $\tau = 1{,}372$). On all 300 certified knots, the certified volume upper end also lies well below the nerve bound $52G \approx 47.6302$, confirming that the 658 residual rows reflect looseness of the upper bounds rather than near-violations of (1). (Up to mirror reflection, the 658 rows correspond to 186 diagrams and the 300 knot rows to 76 knots, as noted during internal review.)

Proposition 7 (Eight-Region Elimination and Residual Certification). *Across the* 62 *duality-and-mirror classes of* 8*-edge loopless* 2*-connected plane maps* (56,362 *twist-reduced parts,* 4,867,828 *critical cells at* $c \geq 17$*), Bounds A and B decide* 4,860,736 *cells* (1,666,548 *by the nerve bound and* 3,194,188 *by BCB*)*. Upward row-by-row expansion of the remaining* 7,092 *cells inspects* 2,213,178 *rows with* 0 *cells cut and leaves exactly* 417,798 *residual rows across* 37 *map classes* ($20 \leq c \leq 38$, $13 \leq D_{\max} \leq 18$)*:* 173,628 *knot rows* (*odd* τ) *and* 244,170 *link rows* (*even* τ)*. In the primary SnapPy pass* (*SageMath 10.10, SnapPy 3.3.2, Python 3.12.16;* 3,693.8 s *on* 31 *workers*)*,* 173,627 *of the* 173,628 *knot rows receive certified volume enclosures satisfying* (1)*, with largest volume-to-bound ratio*

$$\frac{\mathrm{vol}_{\mathrm{hi}}}{2\pi\log\tau} = \frac{35.70710403562563}{55.53608101463606} \approx 0.6430$$

at map E8.143*, labelling* `pppppppp`*, sizes* $(4,4,3,3,3,4,4,3)$*,* $c = 28$*,* $\tau = 6{,}897$*. The sole knot row left undecided by the primary pass—map* E8.76*, labelling* `ppppbbpp`*, sizes* $(4,6,4,6,2,2,3,7)$*,* $c = 34$*,* $\tau = 8{,}393$*,* $D_{\max} = 15$*—is certified directly by* 14 *of* 15 *retriangulation jobs across five routes, yielding the common inter-*

val

$$\mathrm{vol}(U) \in [34.06806413878211,\ 34.06806413898797],$$

whose upper end has ratio 0.6001 *against* $2\pi \log 8{,}393 \approx 56.7695$.

At $t = 8$, 413,304 of the 417,798 residual rows (98.92%) concentrate on five map classes: E8.71 (122,732), E8.143 (115,982), E8.102 (76,501), E8.76 (70,480), and E8.29 (27,609), with the remaining 4,494 rows distributed across 32 classes (at most 584 each). Grouped by nerve parameter $D_{\max}$, the residual rows split as 129 at $D = 13$, 238,834 at $D = 14$, 83,856 at $D = 15$, 94,375 at $D = 16$, 364 at $D = 17$, and 240 at $D = 18$. Every certified knot also passed the nerve-bound sanity check (`over: 0`). Table 2 summarizes the $t = 6$, $t = 7$, and $t = 8$ runs, and Figure 3 plots the exact residual crossing-number distributions.

Closing the sole remaining eight-region knot. During the primary $t = 8$ certification pass, every knot was attempted at 53-bit and 212-bit precision across up to 65 randomized triangulations. Only one of the 173,628 knot rows failed to find a positively oriented triangulation in 65 tries: row U on map E8.76 (hexagon 0–1–2–3–4–5 with chords $e_6 = (0,2)$ and $e_7 = (1,4)$, 35 spanning trees, faces $(3,4,4,5)$), labelling `ppppbbpp`, sizes $(4,6,4,6,2,2,3,7)$, $c = 34$, $\tau = 8{,}393$, $D_{\max} = 15$ (where the nerve bound $62G \approx 56.7899$ missed $2\pi \log 8{,}393 \approx 56.7695$ by 0.0203).

This knot was settled independently in two ways:

1. *Fourteen direct SnapPy certificates across five retriangulation routes.* Re-running the original primary seed reproduced the 65 non-geometric attempts byte-for-byte, whereas 14 of 14 jobs across five alternative routes—fresh randomized triangulations (`more`, seeds 5101–5103), iterated random walks (`walk`, seeds 5501–5502), canonical retriangulation (`canon`, seeds 5201–5202), the mirrored diagram (`mirror`, seed 5301), and six simplified Reidemeister-equivalent diagrams (`diagram`, seeds 5401–5406)—all produced certified 53-bit enclosures in 0 to 17 tries. Every pair of intervals intersects, with common intersection

   $$[34.06806413878211,\ 34.06806413898797]$$

   and largest upper end 34.068064449046666. Seven of the 14 certificates operate directly on the original diagram of U without Reidemeister moves or mirroring.
2. *Independent reflection-twin verification.* The vertex involution $\sigma = (0\ 2)(3\ 5)(1)(4)$ of E8.76 exchanges edges $e_0 \leftrightarrow e_3$, $e_1 \leftrightarrow e_2$, and $e_4 \leftrightarrow e_5$, fixes e_6 and e_7, and reverses the cyclic dart rotation at all six vertices (checked explicitly in `recompute.py`), so σ is a reflection of the embedded plane map on S^2. It preserves `ppppbbpp` and maps $(4,6,4,6,2,2,3,7)$ to the twin row W with sizes $(6,4,6,4,2,2,3,7)$ ($\tau = 8{,}393$), whose Tait graph is therefore the mirror image of U's, giving either W or its mirror image (same hyperbolic volume). The primary pass had already certified W on try 0 in

   $$[34.06806413866831,\ 34.06806413910177],$$

   which strictly contains the 14-certificate common interval of U. (Theorem 2 relies on the 14 direct certificates and does not depend on the reflection-twin step.)

Proofs of Theorems 1 and 2. Let K be an alternating hyperbolic knot with $T_J(K) = t \in \{7,8\}$ and $c(K) \geq 17$. By Menasco's and Lackenby's reduction (Section 2), K admits a prime, twist-reduced alternating diagram D with t twist regions and $c(D) = c(K) \geq 17$ crossings, represented up to planar duality and mirror reflection by a twist-reduced configuration (H, s, S_1, a) on one of the 18 ($t = 7$) or 62 ($t = 8$) complete map classes guaranteed by Tutte's rooted-map check (5). Because K is a knot, $\det(K) = \tau(a)$ is odd and K is not the Borromean rings, so both Lemma 3 and Adams's BCB (4) apply to D. By Lemmas 4 and 5, every configuration whose critical cell or upward expansion branch is decided by either bound satisfies (1). By Proposition 6 (for $t = 7$) and Proposition 7 (for $t = 8$), every remaining knot configuration is explicitly enumerated with 0 cells cut and verified by SnapPy's certified volume enclosure inside SageMath to satisfy $\mathrm{vol}_{\mathrm{hi}}(K) < 2\pi \log\det(K)$, establishing Theorems 1 and 2 under the stated SnapPy enclosure assumption. □

Explicitly unsettled boundaries. To maintain strict scope separation, we record the remaining open conjecture and excluded classes explicitly.

Conjecture 8 (Champanerkar–Kofman–Purcell Vol–Det Conjecture and Unsettled Extensions). *Conjecture 1.10 of Champanerkar, Kofman, and Purcell* [5]*—that* $\mathrm{vol}(K) < 2\pi \log\det(K)$ *holds for every alternating hyperbolic knot* K*—remains unsettled for* $T_J(K) \geq 9$ *below the asymptotic thresholds of Burton* [4] *and Egorov–Vesnin* [7] (*a separate nine-region computation has an unresolved review issue and is not claimed here*). *Likewise, the link analogue for alternating hyperbolic links with* $T_J \in \{7,8\}$ (358 *residual link rows at* $t = 7$ *and* 244,170 *at* $t = 8$) *is not settled by the present work.*

Table 2. Summary of plane-map counts, algebraic cell elimination, residual rows, and SnapPy certified volumes across $t = 6$ (regression control), $t = 7$, and $t = 8$ at $c \geq 17$.

t	Tutte $R(t)$	Sensed / Uns.	Classes	Parts	Critical cells	Decided by bounds	Residual rows	Residual knots	Max $\mathrm{vol}_{\mathrm{hi}}/(2\pi \log \tau)$
6	91	16 / 15	9	1,541	54,813	54,813 (100.00%)	0	0	—
7	408	42 / 36	18	5,670	351,593	351,521 (99.98%)	658	300	0.5933 ($c = 23$)
8	1,938	151 / 114	62	56,362	4,867,828	4,860,736 (99.85%)	417,798	173,628	0.6430 ($c = 28$)

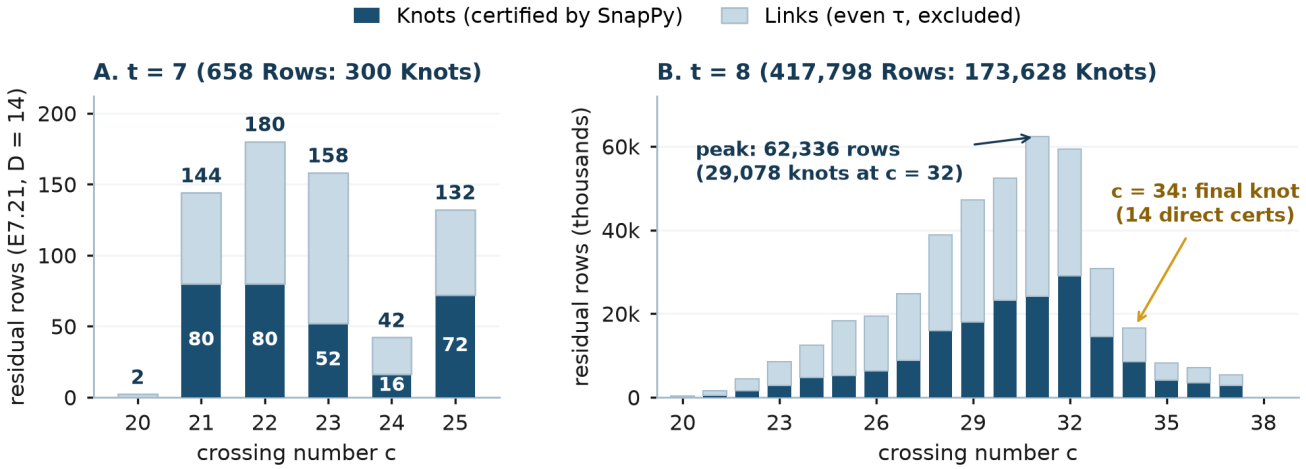

Figure 3. Crossing-number distributions of residual rows left by the nerve bound and Adams's BCB. Panel A ($t = 7$, $c = 20 \ldots 25$): 658 rows on E7.21 ($D = 14$), splitting into 300 certified knots $(0, 80, 80, 52, 16, 72)$ and 358 excluded links (250 two-component, 108 three-component). Panel B ($t = 8$, $c = 20 \ldots 38$): 417,798 rows across 37 map classes, peaking at 62,336 rows ($c = 31$) and 29,078 knots ($c = 32$), splitting into 173,628 certified knots and 244,170 excluded links.

5. FORMAL VERIFICATION & READER'S TRUST BOUNDARY

What You Must Trust to Accept This Paper:

1. **Lean 4 Kernel:** No Lean 4 formalization is claimed in this manuscript.
2. **Written Proofs:** All mathematical arguments rest on standard human-readable proofs.
3. **External Certificates & Written Proofs:** 1 SHA-256-pinned external artifact(s) plus any claims marked Written or Unsettled in Table 3 below.

Reader's Trust-Flow Architecture (Distinct Evidence Paths to Claim Totals)

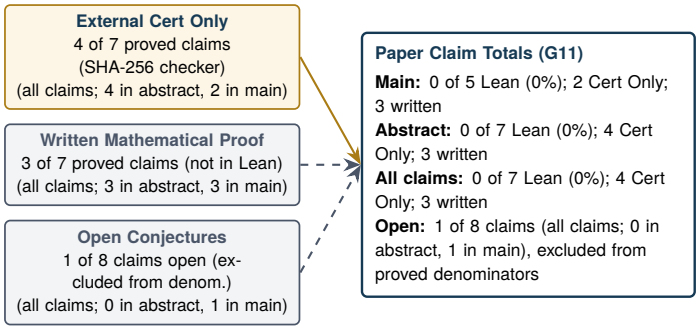

Anti-Shortcut Audit Strip — No-Lean Disclosure

N/A: Lean 4: Not claimed | N/A: sorry / admit: N/A | N/A: native_decide: N/A | N/A: Escape hatches: N/A | N/A: Library coverage: N/A | N/A: Lean fidelity: N/A | WARN: Human referee: pending

Table 3. Per-Claim Reader's Trust Boundary Ledger (G11 Denominators Derived Mechanically).[a]

Paper Claim	Proof Tier	Lean Decl / Artifact	Actual Axioms & Fidelity	Assumptions & What You Must Trust
Thm. 1: Every alternating hyperbolic knot with T_J(K) = 7 and c(K) >= 17 satisfies vol(K) < 2 pi log det(K), given SnapPy verified volume enclosure soundness	Cert Only	recompute.py (aad470ecbd47) [archived; replay pending]	External cert only; fidelity: n/a	No Lean 4 formalization. Combines Lemmas 3-5 (written proofs), complete 7-edge plane-map enumeration matched to Tutte's count (408 rootings) and archived elimination sweep (351,521 of 351,593 critical cells decided), and archived SnapPy verified volume enclosures inside Sage Math 10.10 / SnapPy 3.3.2 for all 300 residual knots (max ratio 0. 5933). Explicitly conditioned on SnapPy's verified computation enclosing the volume of the knot diagram supplied; nothing claimed for links or c <= 16.

Paper Claim	Proof Tier	Lean Decl / Artifact	Actual Axioms & Fidelity	Assumptions & What You Must Trust
Thm. 2: Every alternating hyperbolic knot with T_J(K) = 8 and c(K) >= 17 satisfies vol(K) < 2 pi log det(K), given SnapPy verified volume enclosure soundness	Cert Only	recompute.py (aad470ecbd47) [archived; replay pending]	External cert only; fidelity: n/a	No Lean 4 formalization. Combines Lemmas 3-5 (written proofs), complete 8-edge plane-map enumeration matched to Tutte's count (1,938 rootings) and archived elimination sweep (4,860,736 of 4,867,828 critical cells decided), archived SnapPy enclosures for 173,627 of 173,628 residual knot rows (max ratio 0.6430), and 14 direct SnapPy certificates across five retriangulation routes closing the final knot row (E8.76, c = 34, tau = 8,393), corroborated by an independent reflection twin. Conditioned on SnapPy's verified enclosure soundness; nothing claimed for links or c <= 16.
Lem. 3: General-t nerve upper bound vol(S^3 \ K) < 2(6t - 2 - D_max) G for any prime, twist-reduced alternating hyperbolic link diagram with t >= 3 twist regions	Written	Written proof	Lean: none; fidelity: n/a	Written proof via fully augmented link Dehn-filling monotonicity (Futer-Kalfagianni-Purcell 2019), Agol-D. Thurston right-angled ideal polyhedron decomposition (Lackenby 2004), and orthoscheme / edge-count bound (Atkinson 2009; Alexandrov-Bogachev-Egorov-Vesnin 2023, Lemma 3.2). Thresholds B_t(D) verified to 60 digits in recompute.py. No Lean 4 formalization.
Lem. 4: Weighted spanning-tree determinant lower bounds (Bound A over all trees, Bound B within active-count classes, and rearrangement placement minimization)	Written	Written proof	Lean: none; fidelity: n/a	Elementary written proof via AM-GM and the rearrangement inequality, using det(K) = tau(G) (Stoimenow 2007 [to check], cited via Burton 2018). No Lean 4 formalization.
Lem. 5: Monotonicity of tau(a), critical-cell lowering at c >= 17, and finite termination of upward row expansion under the nerve bound and Adams BCB	Written	Written proof	Lean: none; fidelity: n/a	Written proof from multi-affinity of tau(a) on loopless 2-connected plane maps, invariance of the nerve bound for a_e >= 2, and saturation of Adams's bigon-chain bound (Adams 2017, Theorem 3.1) for twist sizes >= 5. No Lean 4 formalization.
Prop. 6: Seven-region map enumeration (408 Tutte rootings, 18 classes), algebraic elimination of 351,521 of 351,593 critical cells, and SnapPy certification of all 300 residual knots (max ratio 0. 5933)	Cert Only	recompute.py (aad470ecbd47) [archived; replay pending]	External cert only; fidelity: n/a	Archived cloud-box map enumeration, cell/row elimination (0 cells cut, 658 residual rows = 300 knots + 358 links on E7.21 at D = 14), and SnapPy 3.3.2 / SageMath 10.10 volume enclosures; Tutte counts, E7.21 topology/determinants, and tallies independently verified in recompute.py. Conditioned on SnapPy enclosure soundness.

Paper Claim	Proof Tier	Lean Decl / Artifact	Actual Axioms & Fidelity	Assumptions & What You Must Trust
Prop. 7: Eight-region map enumeration (1,938 Tutte rootings, 62 classes), elimination of 4,860,736 of 4,867,828 critical cells, and SnapPy certification of all 173,628 residual knots (173,627 primary + 14 direct certs on final row; max ratio 0.6430)	Cert Only	recompute.py (aad470ecbd47) [archived; replay pending]	External cert only; fidelity: n/a	Archived cloud-box map enumeration, cell/row elimination (0 cells cut, 417,798 residual rows = 173,628 knots + 244,170 links across 37 map classes), primary SnapPy 3.3.2 / SageMath 10.10 pass (173,627 certified), and 14 direct retriangulation certificates on the final knot row (E8.76, c = 34, tau = 8,393); Tutte counts, E8.76 reflection symmetry, determinants, 14-interval intersection, and tallies independently verified in recompute.py. Conditioned on SnapPy enclosure soundness.
Conj. 8: Full CKP Vol-Det conjecture (T_J >= 9 below asymptotic thresholds) and link analogue at T_J in {7, 8}	Unsettled	Open conjecture	Lean: none; fidelity: n/a	Explicitly unsettled open problems excluded from G11 denominators (a separate nine-region computation has an unresolved review issue and is not claimed).

[a] Allowed pure-kernel axioms: `propext`, `Classical.choice`, `Quot.sound`. Actual axioms printed above are read directly from verified outputs. Provenance nonce: ef4d33e737ca | Fidelity SHA-256: c6581501fb88.

6. PRIOR WORK, LITERATURE SEARCH, AND OPEN QUESTIONS

Credited prior work. The Vol–Det conjecture and its experimental check through 16 crossings are due to Champanerkar, Kofman, and Purcell [5]. The volume bounds underlying our reduction are published theorems: Agol and D. Thurston's polyhedral decomposition of alternating links in Lackenby [10], the fully augmented link structure and Dehn-filling monotonicity in Futer, Kalfagianni, and Purcell [8, 9], Atkinson's orthoscheme estimates [3], the right-angled ideal polyhedron edge bound in Alexandrov, Bogachev, Egorov, and Vesnin [2] (Lemma 3.2), Dasbach and Tsvietkova's twist-size bound [6] (Theorem 2.3), and Adams's bigon-chain improvement [1] (Theorem 3.1). On the determinant side, $\det(K) = \tau(G)$ is credited to Stoimenow [12] (`[to check]`, read via [4, 7]), and map completeness rests on Tutte's rooted nonseparable planar map formula [13] (`[to check]`, read via OEIS `A000139`, with `A006402` and `A006403` as cross-checks).

For Vol–Det itself, Burton [4] proved the inequality for 2-bridge links (Theorem 3.5), alternating 3-braids (Theorem 4.1), alternating pretzel links with at most 13 twist columns (§5.1), Montesinos links from $c \geq 3{,}502$ ($t = 7$) and $c \geq 11{,}255$ ($t = 8$) (Corollary 5.2), and general alternating links from $c \geq 16{,}178$ ($t = 7$) and $c \geq 81{,}399$ ($t = 8$) (Theorem 5.1). Egorov and Vesnin [7] sharpened the asymptotic threshold for diagrams with $t(D) > 8$ twist regions (not covering $t = 7$ or $t = 8$). Stanggassinger [11] (unrefereed Zenodo deposit, Section 2 and Remark 2 read; code and logs `[to check]`) checked Vol–Det across all 51,280,967 hyperbolic prime alternating knots through 19 crossings.

Logged prior-work searches and remaining gaps. Four dated search passes were conducted using published terms only: (i) a 20-request sweep across the arXiv API, OpenAlex, Semantic Scholar, and Zenodo; (ii) a 19-query pass on MathSciNet's free MR Lookup; (iii) seven keyed queries on Google Scholar and CORE; and (iv) a five-query Google Scholar sweep on 2026-11-22 (50 returned records). No source settling Vol–Det for alternating hyperbolic knots with 7 or 8 twist regions across $c \geq 17$ crossings was found in the searches logged. Several items remain owed (`[to check]`): full texts beyond title and snippet for the Baykur–Kirby–Ruberman (2026) problem list (`[to check]`), the 2025 Vesnin–Egorov Omsk conference abstract (`[to check]`), and BIRS workshop reports 18W5007 and 25W5497 (`[to check]`); the unshown MathSciNet MR Lookup matches beyond the free three-record cap (15 of 18 under Vesnin, 5 of 8 under Futer, and 1 of 4 under determinant volume links); primary full texts of Tutte [13] (`[to check]`) and Stoimenow [12] (`[to check]`); and a clean re-query of the CORE request that returned HTTP 500.

Open questions. Four concrete follow-ups stand out:

1. *Lean 4 formalization of the reduction:* Formalizing Lemmas 3–5, the plane-map completeness check against (5), and the exact rational/interval elimination of the 351,521 ($t = 7$) and 4,860,736 ($t = 8$) decided cells would move the combinatorial backbone inside a proof assistant, leaving only the finite SnapPy enclosures as external certificates.

2. *Sharper analytical bounds on* E7.21 *and the five dominant* 8*-edge classes:* Because every certified residual knot has volume at most 0.6430 of $2\pi \log \tau$, a modest refinement of the nerve bound (or Adams's face-centered bipyramid bound, Theorem 4.1 of [1]) could eliminate all 300 knots at $t = 7$—and potentially most of the 173,628 at $t = 8$—without any hyperbolic volume computation.
3. *Alternating links at* $t \in \{7, 8\}$*:* Certifying the 358 excluded link rows at $t = 7$ (and 244,170 at $t = 8$) would extend Theorems 1 and 2 from knots to all alternating hyperbolic links.
4. *Nine twist regions and beyond:* Resolving the review gap in the separate $t = 9$ computation, or finding a uniform inductive bound on $\tau(G)$ against the nerve and bigon-chain upper bounds, remains open toward Conjecture 8.

7. DATA AVAILABILITY, REPRODUCIBILITY, AND USE OF AI

All manuscript source files, figure-generation scripts, exact-arithmetic verification code, and trust-boundary ledgers live in `papers/knot-volume-determinant/draft1/`. Running

```
python3 papers/knot-volume-determinant/draft1/recompute.py
```

independently replays Tutte's rooted map counts ($E = 2 \ldots 8$), the 60-digit Catalan constant G and tetrahedral volume v_3, every nerve threshold $B_t(D)$ in Table 1, the worked 7-bond and 8-bond calculations and Section 1 Python snippet, the exact planar rotations, spanning trees, and determinants of E7.21 and E8.76 (including the sphere reflection σ), all archived cell/row tallies, Burton's asymptotic thresholds, and 6/6 negative-mutation controls (saved in `recompute.out`).

The full 7-edge and 8-edge cell elimination sweeps and the 300 + 173,628 certified volume enclosures were produced on cloud compute nodes running SageMath 10.10, SnapPy 3.3.2, and Python 3.12.16; their SHA-256-pinned run receipts and pulled tables are archived in the project research record. Those SnapPy computations are not re-executed by `recompute.py`, and no independent second hyperbolic-volume verifier was run on the residual knot lists; accordingly, Theorems 1 and 2 carry the explicit condition that SnapPy's verified computation encloses the volume of the knot diagram supplied.

AI disclosure and review status. AI research agents built and directed by Tyler B. Hughes generated the mathematical reductions, computer-assisted elimination and certification runs, internal dual-falsifier review checks, figures, and manuscript text. No human mathematician has yet refereed the proof.

Drafted: November 2026 **Updated:** November 24, 2026

REFERENCES

(1) Adams, C. Bipyramids and bounds on volumes of hyperbolic links. *Topology Appl.* **2017**, *222*, 100–114. DOI: 10.1016/j.topol.2017.03.002. arXiv:1511.02372v1.

(2) Alexandrov, S.; Bogachev, N.; Egorov, A.; Vesnin, A. On volumes of hyperbolic right-angled polyhedra. Preprint, **2023**. arXiv:2111.08789v2.

(3) Atkinson, C. K. Volume estimates for equiangular hyperbolic Coxeter polyhedra. *Algebr. Geom. Topol.* **2009**, *9* (2), 1225–1254. DOI: 10.2140/agt.2009.9.1225. arXiv:0804.2682v3.

(4) Burton, S. D. The determinant and volume of 2-bridge links and alternating 3-braids. *New York J. Math.* **2018**, *24*, 293–316. arXiv:1704.02344v1.

(5) Champanerkar, A.; Kofman, I.; Purcell, J. S. Geometrically and diagrammatically maximal knots. *J. Lond. Math. Soc.* (2) **2016**, *94* (3), 883–908. DOI: 10.1112/jlms/jdw062. arXiv:1411.7915v4.

(6) Dasbach, O. T.; Tsvietkova, A. A refined upper bound for the hyperbolic volume of alternating links and the colored Jones polynomial. *Math. Res. Lett.* **2015**, *22* (4), 1047–1060. arXiv:1310.0788v5.

(7) Egorov, A.; Vesnin, A. The Vol-Det Conjecture for highly twisted alternating links. *Math. Notes* **2026**, *119*, 21–28. DOI: 10.1134/S0001434626600274. arXiv:2411.11711v2.

(8) Futer, D.; Kalfagianni, E.; Purcell, J. S. Dehn filling, volume, and the Jones polynomial. *J. Differential Geom.* **2008**, *78* (3), 429–464. arXiv:math/0612138v4.

(9) Futer, D.; Kalfagianni, E.; Purcell, J. S. A survey of hyperbolic knot theory. In *Springer Proc. Math. Stat.* **2019**, *284*, 1–30. DOI: 10.1007/978-3-030-16031-9_1. arXiv:1708.07201v1.

(10) Lackenby, M. The volume of hyperbolic alternating link complements (with an appendix by Ian Agol and Dylan Thurston). *Proc. Lond. Math. Soc.* (3) **2004**, *88* (1), 204–224. DOI: 10.1112/s0024611503014291. arXiv:math/0012185v2.

(11) Stanggassinger, W. A. Vol-Det, Fox, Hoste and a conjecture of Hirasawa–Murasugi for all prime alternating knots with at most 19 crossings. Zenodo Preprint v4, **2026**. DOI: 10.5281/zenodo.23568623.

(12) Stoimenow, A. Graphs, determinants of knots and hyperbolic volume. *Pacific J. Math.* **2007**, *232* (2), 423–451. DOI: 10.2140/pjm.2007.232.423.

(13) Tutte, W. T. A census of planar maps. *Canad. J. Math.* **1963**, *15*, 249–271. DOI: 10.4153/CJM-1963-029-x.